

# Rectangular Chain Packing of Methyl-Branched Paraffins: Persistence of an Interchain Interaction and Forms of Disorder

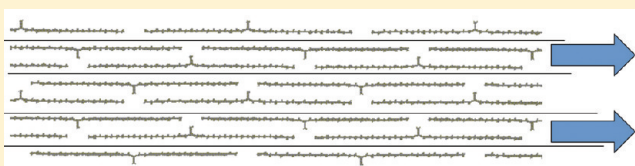
Douglas L. Dorset,<sup>\*,†</sup> Lisa Saunders Baugh,<sup>†</sup> Jun Luo,<sup>‡</sup> and Kenneth J. Shea<sup>‡</sup>

<sup>†</sup>ExxonMobil Research and Engineering, Corporate Strategic Research Laboratory, 1545 Route 22 East, Annandale, New Jersey 08801, United States

<sup>‡</sup>Department of Chemistry, University of California, Irvine, California 92697, United States

**S** Supporting Information

**ABSTRACT:** The rectangular crystal packing of methyl-branched paraffins in their orthorhombic forms is studied systematically by electron diffraction to show that, irrespective of branch position on the chain, a close interaction of chain double rows occurs, placing the branch in the space between two chain ends. If the chain branches occur near the ends, the structure can slowly rearrange into a true bilayer. If the branch occurs near the center, then there are a large number of intermediate “nematocrystalline” disordered forms that are possible before the final ordered layered packing.



## INTRODUCTION

Although normal chain alkanes dominate the composition of most petroleum-based paraffinic waxes, there are cases for polydisperse chain arrays where methyl-branching is an important determinant for the assembly of a waxy solid. Depending on the catalyst used, methyl branches are incorporated into synthetic Fischer–Tropsch waxes,<sup>1,2</sup> thus changing physical properties. A class of “microcrystalline” wax also contains a significant branched chain component.<sup>3–5</sup> Conversion of normal paraffin feedstocks into a desirable lower melting lubricant component is achieved by zeolite-mediated catalysis via creation of *iso*-branched products.<sup>6</sup> Addition of a branched chain component to a waxy fuel mixture may also act as a crystal growth modifier to retard the lateral crystal plate size in cold weather.<sup>7</sup>

It is somewhat surprising that very little substantial crystallographic structural information exists for molecules so chemically simple as the branched paraffins. While the influence of methyl-branching on linear polyethylene crystallization has been often discussed,<sup>8</sup> most information about the effect of such side groups on nonchain-folded molecules has come from the crystallographic study of branched chain fatty acids.<sup>9,10</sup> (As discussed by these authors, the efficient copacking of branches around polymethylene subcells should be similar regardless of functional “headgroups”.) It is generally accepted that, for oligomeric materials, small branches, such as a ketone, or even a secondary alcohol functionality,<sup>11</sup> can be included within the polymethylene subcell packing of the chain stem, whereas methyl groups cannot.

The crystal structure of chiral 1-iodo-3-methyltricosane was reported by Abrahamsson, et al.<sup>12</sup> in 1968. Given the similar van der Waals radii of iodine and the methyl group, this might be a possible isomorphous model for 4-methyltetracosane, except that the mass-loading of the halogen might affect overall molecular vibrations so that a different preferred crystal structure could

result. In the crystal structure of the halogen derivative, the polymethylene chains are tilted and pack as interdigitated bilayers in the orthorhombic perpendicular methylene subcell. The branched chain structure, as a form of “headgroup” region, is sequestered from that of the chain stem packing. For methyl-branching near the chain end in the 3-, 4-, and 5- positions, electron diffraction studies on *rac*-3-methyl tritriacontane (3MeC33), *rac*-3-methyl tetratriacontane (3MeC34), *rac*-4-methyl tetratriacontane (4MeC34), and *rac*-5-methyl tetratriacontane (5MeC34)<sup>13</sup> indicated an intermediate form grown from the melt that does not appear to have a clearly defined lamellar interface. Recent powder X-ray studies of methyl paraffins with branches near the center (viz, 20-methyl nonatriacontane (20MeC39) and 18-methyl pentatriacontane (18MeC35))<sup>14,15</sup> or nearer to the chain end (viz, enantiomorphically pure 9-methyl nonacosane (9MeC29) and 11-methyl heptacosane (11MeC27))<sup>16</sup> indicate the existence of at least two polymorphic forms. To our knowledge there is also no crystal structure reported for an isoparaffin, although *iso*-branched fatty acid crystal structures do exist.<sup>9,10</sup> Preliminary electron diffraction data from *iso*-hexacosane<sup>17</sup> reveal a low temperature rectangular layer (i.e., untilted chain) form utilizing the orthorhombic perpendicular methylene subcell and a higher temperature rotator phase. The end-branched materials are those examined previously but after some aging at room temperature,<sup>13</sup> whereas the center-branched paraffins include the asymmetric *rac*-17-methyl heptatriacontane (17MeC37) and the symmetric 19-methyl heptatriacontane (19MeC37).

**Received:** March 16, 2011

**Revised:** June 1, 2011

**Published:** June 03, 2011

It is also known that, for a given chain length, moving the methyl branch toward the chain center lowers the melting point.<sup>18</sup> In this report, the structures of methyl-branched paraffins are described as the methyl position is moved from the chain end to the chain center.

## EXPERIMENTAL METHODS

**Branched Paraffins.** Samples of 3MeC33, 3MeC34, 4MeC34, and 5MeC34 were originally supplied by Dr. John R. Fryer, Chemistry Department, University of Glasgow, Scotland. Transitions to the rotator phase and the melt, determined by differential scanning calorimetry (DSC), were published in an earlier paper.<sup>13</sup>

Samples of 17MeC37 and 19MeC37 were synthesized as described in a recent paper.<sup>19</sup> (These compounds also serve a biological function as ant “recognition pheromones”.<sup>16,19</sup>) DSC measurements of melting point are shown in Figures S-1 and S-2 (Supporting Information). These measurements were taken at a ramp rate of 10 °C/min using a TA Instruments 2920 calorimeter fitted with a liquid nitrogen cooling accessory.

**Crystallization.** As stated in a previous paper,<sup>13</sup> samples of the branched paraffins with branches near the chain end were originally prepared as dilute solutions in light petroleum and recrystallized by evaporation onto a suitable surface (such as a carbon film-covered 300 mesh Cu transmission electron microscopy (TEM) grid). The solvent used for center-branched paraffins was an isomeric mixture of xylenes. In all cases, epitaxial orientation of these materials was achieved by cooling a comelt with benzoic acid, according to a previously published procedure.<sup>20</sup> It was possible to anneal the samples in the presence of the benzoic acid substrate before this was removed from the branched paraffin by sublimation in vacuo. This annealing step was done on a calibrated controllable hot plate, while the sample assembly (branched paraffin + benzoic acid) was confined between two halves of a previously split mica sheet. Carbon film-covered TEM grids could be added so that epitaxial benzoic acid/paraffin layers would adhere to the grid surface.<sup>21</sup>

**Electron Diffraction.** Original selected area electron diffraction studies<sup>13</sup> of “end-branched” paraffins were carried out at 100 kV with a JEOL JEM-100CX II electron microscope at the Hauptman-Woodward Medical Research Institute in Buffalo, NY. Patterns were recorded on either Kodak DEF-5 or CEA Reflex X-ray film. Further examination of these materials and also the “center-branched” paraffins was carried out at 300 kV with a Philips CM-30 electron microscope. Patterns were recorded on Kodak SO-163 or Biomax MS films. In all cases, radiation damage to the specimens was minimized by use of low electron beam current densities.<sup>21</sup> Diffraction films were digitized on a flat-bed optical scanner, and intensities were extracted from the digital records with the program ELD<sup>22</sup> within the CRISP software package.<sup>23</sup>

**Computations.** Kinematical structure factor calculations via Doyle-Turner<sup>24</sup> electron scattering factors and calculations of potential maps were carried out, respectively, using the programs SF (Moss and Dorset, unpublished) and NIELSAV.<sup>25</sup> Direct methods predictions of crystallographic phases by maximum entropy and likelihood were made using the program MICE.<sup>26</sup> Predictions of molecular packing were made using the Polymorph Predictor module in the Materials Studio 4.2 package (Accelrys, Inc.), first geometrically optimizing constructed molecular models for branched chain paraffins via the program VAMP, before allowing the ensemble to find energy-minimized packing arrays. (The orthorhombic space group chosen, following ref 14 was

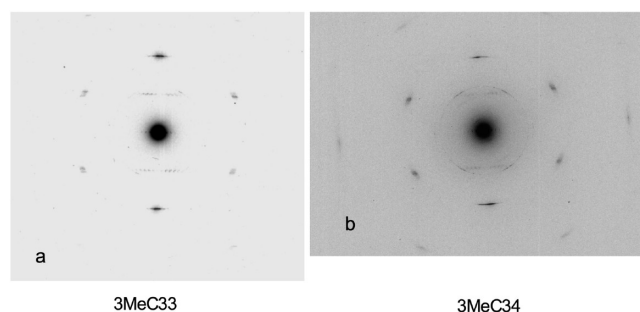


**Figure 1.** Experimental  $0kl$  patterns for ordered methyl-branched paraffins: (a) 3MeC33 and (b) 3MeC34.

$P2_12_12_1$ .) After comparing to other independent determinations, further optimization of the molecular packing geometry was made via the program Forcite within Materials Studio. Simulated electron diffraction patterns from the packing models could be generated with the appropriate module in Cerius<sup>2</sup> (Accelrys, Inc.) to allow comparison to experimental data.

## RESULTS

**End-Branched Paraffins.** As was realized in previous work,<sup>13</sup> the layer packing of all four investigated materials (viz, 3MeC33, 3MeC34, 4MeC34, and 5MeC34) is rectangular (i.e., chains are untilted) and electron diffraction patterns from them are characteristic of the orthorhombic perpendicular methylene subcell.<sup>17</sup> (This subcell is the crystal structure of polyethylene<sup>27,28</sup> in space group  $Pnam$ , where  $a = 7.48$ ,  $b = 4.97$ , and  $c = 2.55$  Å, where the  $c$ -axis is parallel to the long chain axis.) Following the hierarchical scheme of ordering paraffin structures (Figure S-3) crystallized from the melt, followed by annealing,<sup>29</sup> the initial electron diffraction patterns observed from epitaxially oriented 3MeC33, 3MeC34, 4MeC34, and 5MeC34 essentially resembled those from bridged linear wax systems.<sup>17</sup> That is to say, chain ends projecting into apposing layer surfaces prevent a well-defined lamellar packing. This intermediate structure is betrayed by the appearance of the  $0kl$  patterns (see Figure S-3). The “polyethylene” portion of the  $0kl$  pattern with the most intense reflections betrayed no split peaks. Otherwise a single ( $00l$ ) reflection could be observed, indicating nascent layer formation, but not true lamellar separation.<sup>17</sup>

Within the time frame of the original experiments begun over a decade ago,<sup>13</sup> another pattern, which appears after annealing, was observed for 3MeC33 after equilibration at room temperature for 5 months (Figure 1a). The same sort of pattern has been seen frequently in subsequent years for annealed 3MeC34 (Figure 1b) as well as for 5MeC34, again, after allowing the original oriented samples to equilibrate at room temperature. The slow transformation to a more stable crystal packing was, therefore, monitored over 10+ years. In the emergent  $0kl$  patterns, there are now more orders observed for the inner ( $00l$ ) row; the intense polyethylene ( $01l$ ) reflection is elongated and sometimes split (indicative of lamellar separation, see Figure S-3 for analogy to an  $n$ -paraffin); there is also an inner row of ( $01l$ ) reflections never seen before for any  $n$ -paraffin system.<sup>17</sup> Again, original patterns from materials freshly crystallized from the melt<sup>13</sup> do not contain the ( $01l$ ) features shown in Figure 1.

Attempts to determine the emergent packing array with the Materials Studio Polymorph Predictor were often fruitless.

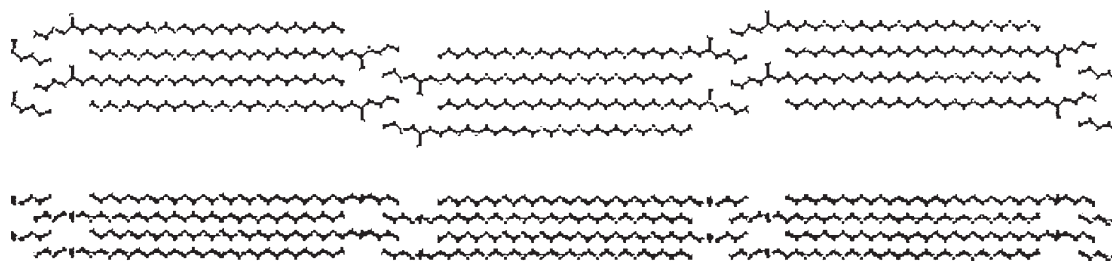


**Figure 2.** Model for 5MeC34 found by Polymorph Predictor. Top: projection down a 5.0 Å axis; bottom: projection down a 7.5 Å axis.

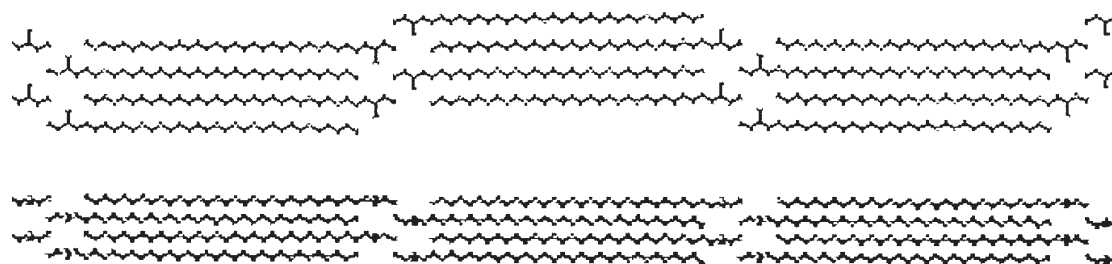


**Figure 3.** Structural model for 3MeC34, derived from Figure 2. The lower projection will generate the pattern in Figure 4. Top: projection down a 5.0 Å axis; bottom: projection down a 7.5 Å axis.

Culling structures that packed in rectangular layers found that most of them did not reproduce the orthorhombic perpendicular methylene subcell packing or the unit cell dimensions expected from the electron diffraction data from these materials. Eventually a model was found for 5MeC34 with an approximate lateral methylene chain arrangement ( $6.97 \times 4.74$  Å; adjacent chain planes perpendicular) with a bilayer structure with long dimension (95 Å) approximately twice found for the C34 members.<sup>13</sup> (Previous  $d_{002}$  measurements for 3MeC34 yielded  $47.80 \pm 0.30$  Å; current measurements give  $46.96 \pm 0.50$  Å.) VAMP-optimized chains tended to have a somewhat bowed molecular structure. If this model were constrained to more typical measured cell dimensions ( $7.42 \times 5.00 \times 94.95$  Å) using the Forcite geometrical optimization, the chains became less bowed, and the structural model (Figure 2) produced an electron diffraction pattern with recognizable features, comparable to the observed patterns in Figure 1. A model for the 3MeC34 homologue could be easily constructed from this result (Figure 3) and with the correct diffraction pattern (Figure 4). It is clear that a true bilayer structure can emerge from this chain array. Although it is not entirely evident from the Cerius<sup>2</sup> pattern simulation (Figure 4), other salient diffraction details are observed in a structure factor calculation as outlined in Table S1, and these match the indices and relative intensities of major reflections observed in the  $0kl$  diffraction pattern (Figure 1). Note that, in Figures 2 and 3, the methyl groups are lodged within gaps provided by chain ends of the next layer.

**Middle-Branched Paraffins.** As also discussed in the earlier powder X-ray study of structural homologues 20MeC39 and 18MeC35,<sup>14,15</sup> the major polymorphic form of paraffins with branches near the center is an oblique layer packing, perhaps with the  $T_{||}$  subcell packing. The low energy form of 20MeC39 was modeled<sup>14</sup> in space group  $P\bar{1}$ , where  $a = 10.5$ ,  $b = 4.70$ ,  $c = 51.76$  Å,  $\alpha = 72.6^\circ$ ,  $\beta = 68.0^\circ$ , and  $\gamma = 65.0^\circ$ . In this study of solution crystallized samples, particularly of the 17MeC37, a strong

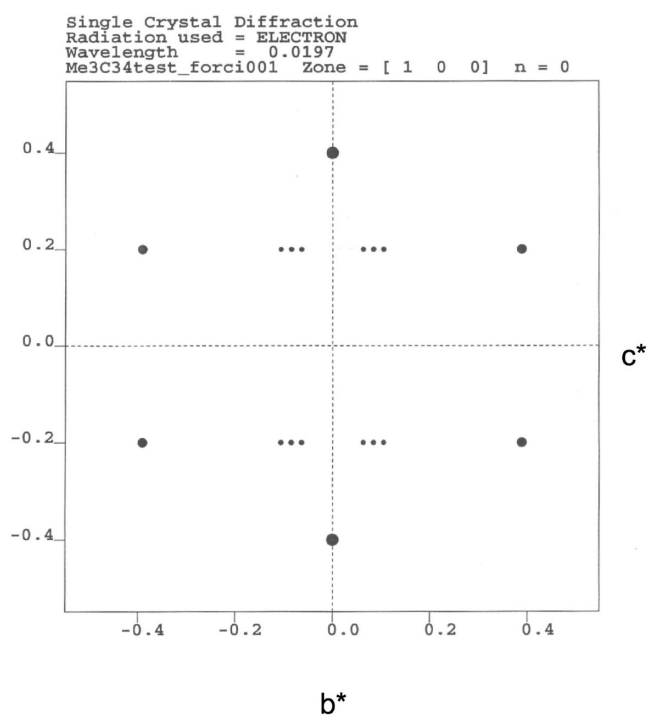


**Figure 4.** The  $0kl$  pattern predicted for 3MeC34. (See Table S1 for a more detailed list of reflections.)

diagonal reciprocal lattice row with spacing  $d = 4.60(5)$  Å is often observed, similar to the characteristic electron diffraction patterns from triglycerides packing with the same triclinic parallel methylene subcell,<sup>30</sup> where  $d_{110} = 4.54(2)$  Å. An oblique projection of the chain packing is also observed occasionally for epitaxially oriented 19MeC37 (Figure S-4), containing  $(00l)$  reflections with a spacing near 26 Å (compensating for the  $69.2^\circ$  reciprocal angle).



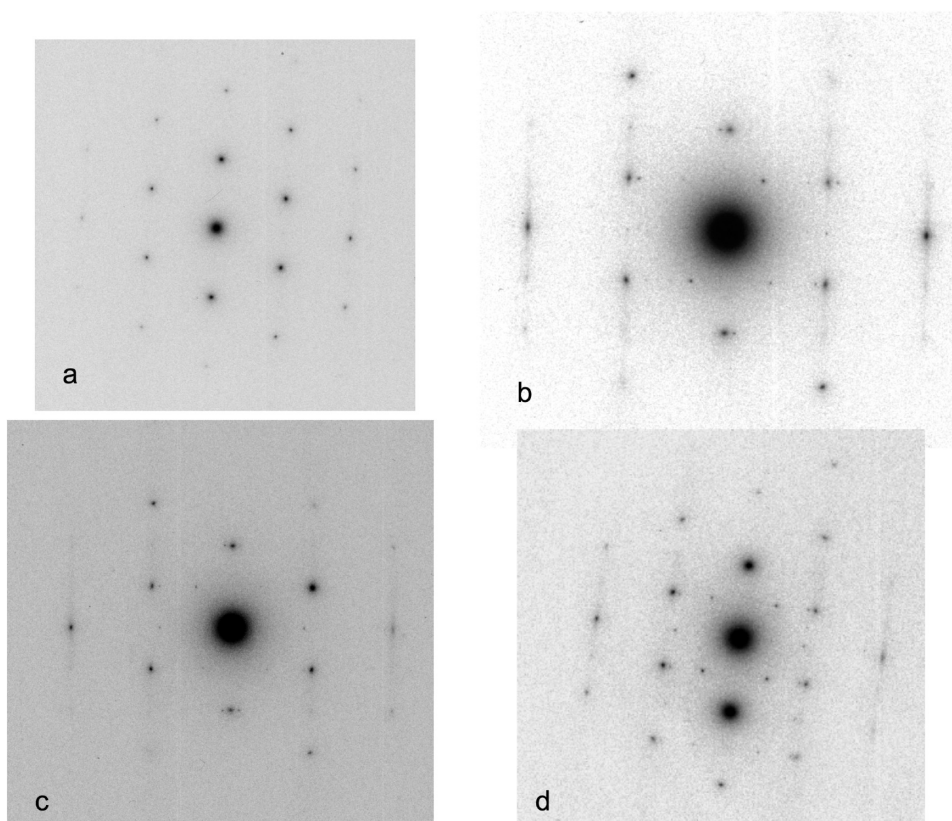


**Figure 5.** Variety of  $(0kl)$  patterns from 19MeC37 in rectangular chain packing. (a) Polyethylene-like (see ref 28). (b) Satellite spots for polyethylene (020) and (011). (c) Satellite spots for (020). (d) Satellite spots for polyethylene (011).

Agreeing also with the earlier powder diffraction studies of the homologous 20MeC39,<sup>14</sup> there is also a rectangular layer polymorph. From solution crystallized samples, the patterns, viewing down the chain axes (Figure S-5b) from 19MeC37 indicate *cm*m symmetry rather than the *pgg* of the orthorhombic perpendicular subcell (Figure S-5a) with lateral cell dimensions  $7.55(5) \times 5.02(5)$  Å. Although a similar pattern was also observed for 17MeC37, it was not as commonly encountered.

Epitaxial orientation on benzoic acid expresses mostly the rectangular layer (presumably orthorhombic) polymorph. Sometimes  $(0kl)$  patterns closely resembling those from polyethylene are observed (Figure 5a). Attempts were made to form a more ordered chain packing array by, e.g., annealing 19MeC37 at 35 °C for 8 h. Patterns with a bewildering variety of additional reflections were observed in this case; for example, those with some inner  $(01l)$  “lamellar” reflections; those with satellites to the intense  $(01l)$  polyethylene reflection, but on both sides and not necessarily betraying rectangular symmetry; those with satellites to the strong  $(020)$  reflection and also not necessarily rectangularly symmetrical; or some combination of all of these (Figure 5). Curiously, inner  $(00l)$  layer reflections were never seen. Using available satellite reflection positions for pattern indexing, a frequently observed spacing is 25.5 Å, closely agreeing with the mean value given in the literature<sup>14,15</sup> between 18MeC35 and 20-methylnonatriacontane (20MeC37). Although the 17MeC37 isomer was not so extensively studied, diffraction from epitaxial samples was quite similar.

Attempts were made to find a suitable packing array using the Polymorph Predictor module within Materials Studio, but no rectangular chain packing model was found that also incorporated

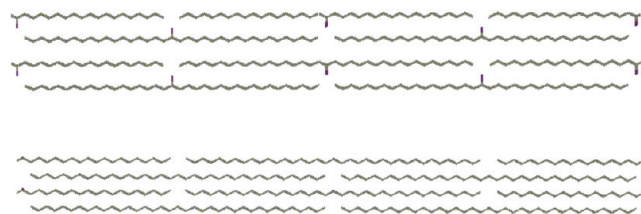


**Figure 6.** Ordered chain packing model for 19MeC37 (analogous to 20MeC39<sup>14</sup>). Top: projection down a 5.0 Å axis; bottom: projection down a 7.5 Å axis.

the orthorhombic perpendicular polymethylene packing. Using a model derived from the orthorhombic form of homologous 20MeC39 (Figure 6), it is clear that a perfectly aligned chain array should generate inner  $(00l)$  lamellar reflections in its  $(0kl)$  pattern. Again, the  $(00l)$  layer reflections from 19MeC37 have not been observed yet for the rectangular packing. Direct methods phase assignment to observed  $(0kl)$  reflections reveals that the methyl branching position should be distributed around the mean position in the model above. As suggested by parallel chain packing arrays from the Polymorph Predictor (Figure 7), a pair of interacting methyl-branched chains always seems to be closely associated in double molecular rows. Again, methyl groups are accommodated in the gap provided by chain ends of the next layer. These double rows of molecules seem to be locked into a stable structural array. However, by analogy to *n*-paraffins (Figure S-3), there is another surface where the chains can slip by one another along their length. Thus, a “nematocrystalline” array of chains with no well-defined nascent layer formation would

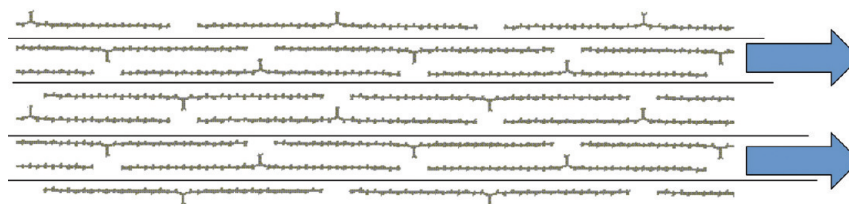


**Figure 7.** Disordered chain packing for 19MeC37 suggested by Polymorph Predictor. This only shows the form of interlayer interactions. (Compare to Figure 6, top.) Arrows indicate that neighboring chain double layers can slide by the central fixed double layer to generate an array of intermediate nematocrystalline chain packings.

account for a variety of diffraction patterns, some deviating from the rectangular symmetry expected for this projection. For example, a broad, equally weighted distribution of methyl branches in a disordered packing of longitudinally displaced double chain rows will lead to a pattern without strong lamellar (00 $l$ ) reflections.

## DISCUSSION

This is the first systematic crystallographic study of chain packing in methyl-branched paraffins. Electron diffraction provides single crystal data in views down and onto the chain axes so that modeling of crystal structures can be placed on a firmer experimental basis than is possible with the use of overlapped powder diffraction information.<sup>14–16</sup> While structural models from two powder diffraction studies make geometrical sense,<sup>14,15</sup> a more recent suggestion of a “paper-clip” chain conformation in other branched paraffin crystal structures<sup>16</sup> does not.

It is clear that the orthorhombic crystal structures of methyl-branched paraffins all share a common feature, irrespective of where the branch occurs on the chain. The fundamental intermolecular association occurs among double chain rows, accommodating the methyl branch within a gap between chain ends of the apposing molecular row. In this regard, the crystal structure model of Yamamoto, et al.,<sup>14</sup> appears to be correct. However, particularly when crystallized from the melt, there is considerable freedom for these double rows to slide past one another, by analogy to the nematocrystalline structure of normal  $n$ -paraffins.<sup>17</sup> Intermediate disordered forms of these materials will appear, effectively leading to a random distribution of methyl-positions along the chain in an average unit cell.

When the chain branch appears near the chain end, the structure can eventually rearrange itself to recrystallize into a true lamellar packing. (No evidence is found, however, for an isomorphous structure analogous to the halogen analogue described by Abrahamsson et al.<sup>12</sup>) Creation of individual lamellae also implies a relaxation of conformational geometry of chain segments near the interface, and the unit cell repeat is no longer an integral multiple of the methylene subcell repeat along  $c_s = 2.55$  Å (corresponding to the chain axis repeat distance of polyethylene). This resolves an open question from our earlier study<sup>13</sup> about the nature of the emergent chain layer interface. When the chain branching occurs near the center, this rearrangement to an ordered structure is not so easily accomplished. Even in the ordered structure suggested by Yamamoto, et al.,<sup>14</sup> the unit cell long dimension is always an integral multiple of the methylene subcell repeat, because there is never an interlamellar gap.

Obviously the preferred, low-energy polymorph of these branched paraffins also depends on the position of the branching. For the end-branched materials, a rectangular layer packing seems to be retained whereas, for the middle-branched examples,

an oblique layer packing is preferred. Evidence for the latter oblique chain packing has, in fact, been observed in electron diffraction studies of solution-crystallized material (major form) as well as epitaxially oriented material (minor form). The frequency of polymorph occurrence is also a function of the crystallization procedure; epitaxial growth tends to prefer higher energy polymorphs.<sup>17</sup> The instability of the rectangular chain packing in center-branched paraffins may result from steric effects around the methyl branch. The  $cm\bar{m}$  symmetry of the methylene chain subcell (Figure S-5b) also indicates some average conformational disorder of the chain, perhaps a precursor to a rotator phase.

From these structures, it is also clear how branched-chain paraffins might function as growth modifiers for waxy crudes or fuels. As would be expected, it is known that these branched compounds form eutectic solids with the normal paraffins.<sup>14</sup> However, the lateral chain packing of both is quite similar, e.g., in chain tilt and type of methylene subcell packing. If a normal paraffin crystallizes in its characteristic orthorhombic layer packing, the branched paraffins can associate with the growing normal paraffin crystal face through chain surfaces that do not contain branch protrusions. Further growth of the normal paraffin is therefore retarded since deposition of other paraffin molecules is hindered by the branch, i. e., the action of a typical growth poison.

## CONCLUSIONS

This first comparative study of end- and middle-methyl-branched long chain paraffins in their rectangular polymorphs, based on single crystal diffraction data, reveals that certain general packing principles are preserved. That is, the methyl branch is always accommodated within gaps provided by chain ends. Disorder mechanisms require that pairs of locked chain layers slide past one another to create a variety of nematocrystalline arrays.

## ASSOCIATED CONTENT

**S Supporting Information.** Structure factors for 3MeC34; DSC scans from 17MeC37 and 19MeC37; packing arrangements for linear chain paraffins; additional electron diffraction patterns from 19MeC37 and 3MeC34. This material is available free of charge via the Internet at <http://pubs.acs.org>.

## AUTHOR INFORMATION

### Corresponding Author

\*Retired. Current address: Wessex Transforms, 475 Ellis Road, Milford, NJ 08848. E-mail: [wessex9t@yahoo.com](mailto:wessex9t@yahoo.com).

## ■ ACKNOWLEDGMENT

J.L. and K.J.S. would like to thank Ms. Kristin L. Kahale for assistance with synthesis of the hydrocarbon molecules 17MeC37 and 19MeC39. Initial work on the end-branched paraffins was carried out by D.L.D. at the Hauptman-Woodward Medical Research Institute, in Buffalo, NY, and was supported by a grant from the National Science Foundation (CHE-9730317), which is still gratefully acknowledged.

## ■ REFERENCES

- (1) LeRoux, J. H.; Dry, J. J. *Appl. Chem. Biotechnol.* **1972**, *22*, 719–726.
- (2) Stenger, H. G.; Johnson, H. E.; Satterfield, C. N. *J. Catal.* **1984**, *86*, 477–480.
- (3) Musser, B. J.; Kilpatrick, P. K. *Energy Fuels* **1998**, *12*, 715–725.
- (4) Tuttle, J. B. *Petroleum Products Handbook*; Guthrie, V. B., Ed.; McGraw-Hill: New York, 1960; Chapter 10.
- (5) Edwards, R. T. *Ind. Eng. Chem.* **1957**, *49*, 750–757.
- (6) Sequeira, A. *Lubricant Base Oil and Wax Processing*; Marcel Dekker: New York, 1994.
- (7) Petitjean, D.; Schmitt, J. F.; Laine, V.; Bouroukba, M.; Cunat, C.; Dirand, M. *Energy Fuels* **2008**, *22*, 697–701.
- (8) Farmer, B. L.; Eby, R. K. *Polymer* **1979**, *20*, 363–366.
- (9) Abrahamsson, S. *Ark. Kemi* **1959**, *14*, 65–83.
- (10) Abrahamsson, S.; Fischmeister, I. *Ark. Kemi* **1959**, *14*, 57–63.
- (11) Welsh, H. K. *Acta Crystallogr.* **1956**, *9*, 89–90.
- (12) Abrahamsson, S.; Innes, M.; Nilsson, B. *Ark. Kemi* **1968**, *30*, 173–182.
- (13) Dorset, D. L. *Energy Fuels* **2000**, *14*, 685–691.
- (14) Yamamoto, H.; Nemoto, N.; Tashiro, K. *J. Phys. Chem. B* **2004**, *108*, 5827–5835.
- (15) Ikedou, K.; Yamamoto, H.; Nagashima, H.; Nemoto, N.; Tashiro, K. *J. Phys. Chem. B* **2005**, *109*, 10668–10675.
- (16) Brunelli, M.; Fitch, A. N.; Brooks, L.; Jones, G. R. *Acta Crystallogr., Sect. A* **2009**, *65*, s273.
- (17) Dorset, D. L. *Crystallography of the Polymethylene Chain*; Oxford University Press: Oxford, U.K., 2005.
- (18) Warth, A. H. *The Chemistry and Technology of Waxes*; Reinhold: New York, 1947; p 7.
- (19) Brandt, M.; van Wilgenburg, E.; Sulc, R.; Shea, K. J.; Tsutsui, N. D. *BMC Biol.* **2009**, *7*, 71 (9 pages, electronic journal).
- (20) Wittmann, J. C.; Hodge, A. M.; Lotz, B. J. *Polym. Sci., Part B: Polym. Phys.* **1983**, *21*, 2495–2509.
- (21) Dorset, D. L. *Structural Electron Crystallography*; Plenum: New York, NY, 1995.
- (22) Zou, X. D.; Sukharev, Yu.; Hovmöller, S. *Ultramicroscopy* **1993**, *52*, 436–444.
- (23) Hovmöller, S. *Ultramicroscopy* **1992**, *41*, 121–135.
- (24) Doyle, P. A.; Turner, P. S. *Acta Crystallogr., Sect. A* **1968**, *24*, 390–397.
- (25) Hansen, N. K.; Coppens, P. *Acta Crystallogr., Sect. A* **1978**, *34*, 909–921.
- (26) Gilmore, C. J.; Bricogne, G.; Bannister, C. *Acta Crystallogr., Sect. A* **1990**, *46*, 297–308.
- (27) Bunn, C. W. *Trans. Faraday Soc.* **1939**, *35*, 482–491.
- (28) Hu, H.; Dorset, D. L. *Acta Crystallogr., Sect. B* **1989**, *45*, 283–290.
- (29) Zhang, W. P.; Dorset, D. L. *J. Polym. Sci., Part B: Polym. Phys.* **1990**, *28*, 1223–1232.
- (30) Dorset, D. L.; Hancock, A. J. *Z. Naturforsch.* **1977**, *32c*, 573–580.